Available online at www.sciencedirect.com

ScienceDirect

Journal of the European Ceramic Society 29 (2009) 347–353

www.elsevier.com/locate/jeurceramsoc

Thermal conductivity of porous alumina ceramics prepared using starch as a pore-forming agent

Zuzana Živcová[a], Eva Gregorová[a], Willi Pabst[a,*], David S. Smith[b], Aurélie Michot[b], Céline Poulier[b]

[a] *Department of Glass and Ceramics, Institute of Chemical Technology, Prague (ICT Prague), Technická 5, 166 28 Prague 6, Czech Republic*

[b] *Groupe d'Etude des Matériaux Hétérogènes, École Nationale Supérieure de Céramique Industrielle (ENSCI), 47-73, Avenue Albert Thomas, 87065 Limoges Cedex, France*

Received 28 April 2008; received in revised form 5 June 2008; accepted 17 June 2008
Available online 3 August 2008

Abstract

The thermal conductivity of porous alumina ceramics prepared using different types of starch (potato, wheat, corn, and rice starch) as pore-forming agents is investigated from room temperature up to 500 °C. The temperature dependence measured for alumina ceramics of different porosity (in the range 6–47%) is fitted with second-order polynomials and $1/T$-type relations, and compared to available literature data for dense alumina. It is found that the porosity dependence of the relative thermal conductivity $k_r = k/k_0$ is well described by a modified exponential relation of the form $k_r = \exp(-1.5\phi/(1-\phi))$, where ϕ is the porosity. This finding is in agreement with other literature data and seems to indicate a common feature of all porous materials with microstructures resulting from fugitive pore-forming agents.

Keywords: Microstructure-final; Porosity; Thermal conductivity; Al_2O_3; Starch-consolidation casting

1. Introduction

Porous ceramics are widely used for a variety of applications, including burners, thermal barrier coatings and insulating layers.[1,2] Apart from these specific applications, however, the effective thermal conductivity of ceramics (which are usually porous to a certain extent) is of general interest, since it may significantly influence other properties such as thermal shock resistance and may exhibit certain features, in particular a porosity dependence, analogous to other properties, e.g. electrical conductivity or elastic moduli.[3–7] In particular, it has been shown recently that the modified exponential relation proposed by Pabst and Gregorová for the description of the porosity dependence of the Young's modulus[8–11] may also be used, with appropriate modification of the numerical coefficient, for the porosity dependence of the thermal conductivity.[12,13]

The use of pore-forming agents is one of the frequently used methods to produce porous ceramics with controlled microstructure (porosity and pore size).[14–16] During heating up to the final firing temperature of the ceramics, these pore-forming agents are burnt out, leaving void pores in the ceramic. Among the various pore-forming agents, those of biological origin have gained a prominent position, in particular starch.[19–40] They are cheap, non-toxic, environmentally friendly and exhibit defect-free burnout between approximately 300 and 600 °C, with the pore sizes achievable with commercial starch types ranging from approximately 5 μm (for rice starch) to approximately 50 μm for potato starch.[41] Starch can be used as a mere pore-forming agent, e.g. as an additive in traditional slip casting (TSC) or it may be used as a combined pore-forming and body-forming agent (consolidating agent) in so-called starch consolidation or starch-consolidation casting (SCC).[17,18,21–24,34,38,40]

Inspite of the great practical and theoretical importance of the thermal conductivity of porous ceramics, however, systematic investigations of the combined temperature and porosity dependence of thermal conductivity seem to be very rare. In particular, to the best of our knowledge there is no such investiga-

---

* Corresponding author.
E-mail address: pabstw@vscht.cz (W. Pabst).

0955-2219/$ – see front matter © 2008 Elsevier Ltd. All rights reserved.
doi:10.1016/j.jeurceramsoc.2008.06.018

tion for ceramic materials produced with fugitive pore-forming agents, i.e. for microstructures with convex pore shape (essentially matrix-inclusion type microstructures). It is the purpose of this paper to fill this gap. Although focused on alumina ceramics prepared with starch, we would like to emphasize in advance that the results of this paper should essentially be valid for all ceramic materials prepared with pore-forming agents of convex shape, as long as conduction is the dominant heat transfer mechanism.

2. Theoretical

Heat transfer in porous (and cellular) media generally occurs by three mechanisms: conduction, convection and radiation. In many cases, however, the latter two can be neglected. Convection has to be taken into account when the Grashof number, defined as

$$Gr = \frac{g\beta\,\Delta T\,D^3\rho^2}{\eta^2}, \tag{1}$$

exceeds a value of 1000, where $g = 9.81\,\text{m/s}^2$ is the gravitational acceleration, β the volumetric thermal expansion coefficient of the pore gas (considered to be an ideal gas, i.e. $\beta = 1/\vartheta$, with ϑ being the absolute Kelvin temperature), ΔT the temperature difference across one pore, D the pore size (diameter) and ρ and η the density and viscosity of the gas, respectively.[42] Inserting plausible estimates for the variables, corresponding to air at 1 atmosphere and room temperature (i.e. $\rho = 1\,\text{kg/m}^3$, $\eta = 2\times 10^{-5}$ Pas) the critical pore size is $L_{\text{crit}} = 10$ mm for a temperature difference of 10 °C (additionally, of course, for convection to take place, the pores have to be interconnected and open, i.e. accessible from the surface of the body). Since the pore size considered in this paper is below 100 μm (of order tens of micrometers and below), convection can clearly be ignored.

As far as radiation is concerned, its influence can be assessed using the Stefan–Boltzmann radiation law.[43] More specifically, radiation is negligible compared to conduction when the dimensionless ratio

$$\frac{4\gamma\varepsilon\sigma D\vartheta^3}{k_0} \tag{2}$$

is much smaller than unity (≪1). In this ratio γ is a geometric factor of order unity (2/3 for spherical pores), ε the emissivity of the pore surface material (0.38 ± 0.10 for alumina), σ the Stefan–Boltzmann radiation constant ($5.67\times 10^{-8}\,\text{W/m}^2\,\text{K}^4$), D the pore size (diameter, in this work, <100 μm), ϑ the average Kelvin temperature and k_0 the conductivity of the solid phase.[44] Inserting these values one obtains at 500 °C a radiation contribution of 2.66×10^{-3} W/mK, which is clearly negligible with respect to the thermal conductivity of the solid phase (dense alumina) which is approximately 12 W/mK at 500 °C.[45]

When convection and radiation are negligible, heat transfer is governed by the constitutive equation

$$\mathbf{q} = -k\,\text{grad}\,T \tag{3}$$

(Fourier's law), where **q** is the heat flux vector, grad T the temperature gradient and k the thermal conductivity. Of course, in the case of heterogeneous (e.g. porous) materials **q** and grad T have to be considered as volumetrically averaged quantities and k has to be interpreted as an effective thermal conductivity.[3,4,45] Since porous materials in general can be considered as a special case of composites, their effective thermal conductivity is principally bounded by the Wiener bounds or, if the microstructure is isotropic, by the Hashin–Shtrikman bounds.[3,4,12,45] In many cases, however, the thermal conductivity of the pore phase is negligible compared to the thermal conductivity of the solid phase. This is certainly the case for porous alumina ceramics, since the thermal conductivity of dense high-purity alumina with a grain size >1 μm is approximately 33 W/mK at room temperature and approximately 12 W/mK at 500 °C,[45] while the thermal conductivity of air at atmospheric pressure is approximately 0.025 W/mK at room temperature and approximately 0.050 W/mK at 500 °C.[46]

Thus, neglecting the thermal conductivity of the gas phase, i.e. considering the pores as vacuous voids, the lower micromechanical bounds degenerate to zero identically and the Wiener and Hashin–Strikman upper bounds can be written as[45]

$$k_{\text{r}} = 1 - \phi \tag{4}$$

and

$$k_{\text{r}} = \frac{1-\phi}{1+(\phi/2)}, \tag{5}$$

respectively, where ϕ is the porosity (i.e. the volume fraction of voids), and $k_{\text{r}} = k/k_0$ is the relative thermal conductivity, with k denoting the effective thermal conductivity of the porous material and k_0 denoting the thermal conductivity of the solid phase. Since the lower bounds fail altogether, it is clear that any useful prediction of the porosity dependence of thermal conductivity has to be based on model relations. The most important model relations for pores of isometric shape have been critically reviewed in a recent monograph chapter.[45] As a main result, it may be said that the popular power-law relation (differential scheme prediction)

$$k_{\text{r}} = (1-\phi)^{3/2} \tag{6}$$

is rather close to the Hashin–Shtrikman upper bound, while the self-consistent scheme prediction (going back to Landauer[47] and Bruggeman[48]) reduces to the linear relation

$$k_{\text{r}} = 1 - \frac{3}{2}\phi \tag{7}$$

(also called non-interaction approximation or dilute limit approximation) and predicts a finite (but spurious) percolation threshold in this case (viz. pores with zero conductivity). The only predictive non-linear relation which does not violate physical principles (in particular, does not exceed the upper Hashin–Shtrikman bound), is the modified exponential relation

$$k_{\text{r}} = \exp\left(\frac{-(3/2)\phi}{1-\phi}\right), \tag{8}$$

which has been originally proposed (with the appropriate coefficient 2 instead of 3/2) to describe the porosity dependence of the Young's modulus[49] and can be derived using a functional equation approach.[13,50] Recently, for the Young's modulus, the form of this modified exponential relation has been attributed to a high degree of disorder in the pore space,[51] and an analogous interpretation may be expected to apply in the conductivity case.

Apart from the dependence of the effective (or relative) thermal conductivity of the porous material on the microstructure (in particular, porosity), the solid conductivity k_0 is a function of temperature and grain size. From the viewpoint of theory (which considers thermal conductivity to be governed by phonon scattering processes[52]), the thermal conductivity of crystalline solids should decrease (the decrease being inversely proportional to the absolute Kelvin temperature T),

$$k_0 = A + \frac{B}{T}, \tag{9}$$

while for glasses (and highly defective solids) the thermal conductivity (which is typically much lower at room temperature than for the corresponding crystalline solids) should change less and typically according to a linear law of the form $k_0 = C + DT$.[53,54] For ceramic materials with glassy phase boundaries combinations of these two relations have successfully been used, but in many cases purely empirical relations give better fits to measured data.[45,55,56] The grain size dependence of the thermal conductivity has been investigated in great detail for various ceramics in several papers.[57–60] Note however, that this influence cancels out when taking conductivity ratios and is thus of no concern when relative conductivities are considered (provided the grain size remains constant for samples of different porosity).

3. Experimental

3.1. Materials and sample preparation

The materials used in this work are submicron alumina powder (CT 3000 SG, Almatis, Germany) with a median particle size of approximately 0.8 µm and a purity of approximately 99.8% (all α-Al_2O_3), as well as different types of starch:

- Rice starch (Remy FG, Remy Industries NV, Belgium)
- Corn starch (Gustin, Dr. Oetker a.s., Czech Republic)
- Wheat starch (Psenicny Skrob, Amylon a.s., Czech Republic)
- Potato starch (Solamyl, Natura a.s., Czech Republic)

Porous alumina ceramics have been produced by two variants of slip casting:

- Traditional slip casting (into porous plaster molds): in this method starch is used only as a pore-forming agent and body formation occurs by capillary suction (dewatering through the mold wall);
- Starch-consolidation casting (into non-porous brass molds): in this method starch is used as a combined pore-forming and body forming agent—body formation occurs by starch swelling (and gelatinization) during heating to approximately 80 °C which is accompanied by water absorption from the suspension.

In both cases aqueous suspensions were prepared with 70–80 wt.% alumina, 1 wt.% deflocculant (Dolapix CE64, Zschimmer & Schwarz, Germany) and starch concentrations ranging from 5 to 50 vol.% (related to alumina). Details of the starch granule size (distributions) and shape as well as suspension preparation, casting techniques (TSC and SCC) and resulting microstructures have been published in several papers, to which the reader may refer.[38,41,61,62] After demolding, the sample bodies (cylinders of approximately 7 mm diameter and 80 mm length for SCC and disks with diameter approximately 15 mm for TSC) were dried for 24 h at room temperature, followed by drying at 105 °C to constant mass. Subsequently, the bodies were fired according to a standard schedule (heating rate 2 °C/min, 2 h dwell at 1570 °C). Starch burnout takes place during the heating stage in the temperature range 300–600 °C. Finally, the as-fired cylindrical SCC bodies were saw-cut into disks of approximately 2 mm thickness and both the TSC bodies (disks of approximately 13 mm diameter and 2.5 mm thickness) and the SCC bodies (disks of approximately 6 mm diameter and 2 mm thickness) were covered on one face with a thin graphite layer.

3.2. Principle of measurement and data evaluation

The effective thermal conductivity was measured via the thermal diffusivity using the laser-flash technique,[63,64] with a Nd–glass laser operating at 1.053 µm as the flash source to heat the front face of the disk-shaped specimens (the thin graphite layer helps to avoid the direct propagation of laser radiation through the sample). This laser delivers a standard pulse of 30 J in 450 µs. The absorbed heat diffuses through the sample and the transient back-face temperature is recorded using a liquid-nitrogen-cooled IR detector (Hg–Cd–Te) connected to an amplifier and a storage oscilloscope. All measurements (from room temperature to approximately 500 °C) were made in air. The temperature–time data were analyzed using the Degiovanni method, which takes heat losses into account.[64] Finally, the resulting thermal diffusivity values α were transformed into thermal conductivities using the relation

$$k = \rho c_P \alpha, \tag{10}$$

where ρ is the bulk density of the sample (in our work determined by the Archimedes method) and c_P is the specific heat, for which several empirical approximation formulae are available, the simplest of which is

$$c_\mathrm{P} = 512.6\vartheta^{0.131} \tag{11}$$

for alumina,[45] where ϑ is the temperature value in °C. According to this relation the c_P value of alumina varies between 773 J/kg K at room temperature and 1157 J/kg K at 500 °C.

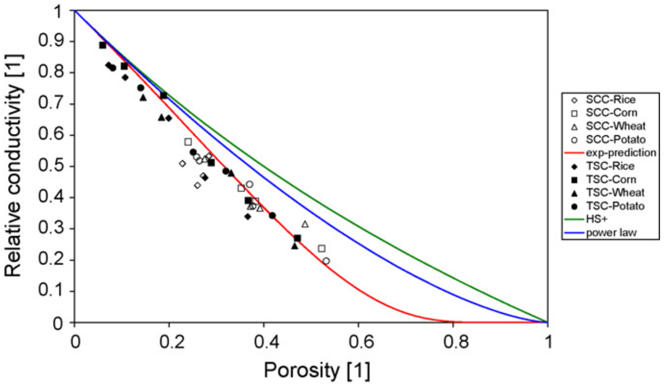

Fig. 1. Porosity dependence of the relative thermal conductivity of alumina ceramics prepared by starch-consolidation casting (empty symbols) and traditional slip casting (full symbols), compared to the HS upper bound (top curve), the power-law relation (middle curve), and the modified exponential relation (bottom curve); experimental data measured in this work.

4. Results and discussion

Fig. 1 shows the relative thermal conductivity $k_r = k/k_0$ of porous alumina ceramics at room temperature in dependence of the porosity. The relative conductivity values have been obtained by dividing the measured effective thermal conductivity k by $k_0 = 33$ W/mK, which is a reasonable value for the thermal conductivity at room temperature of pure dense alumina ceramics.[45] Note that for the relative thermal conductivity the grain size dependence of thermal conductivity[57–60] is irrelevant, since it is cancelled out by taking the conductivity ratio.

It is evident that all measured data are below the upper Hashin–Shtrikman bound (top curve), as required for materials isotropic microstructures in general, and also significantly below the power-law prediction (middle curve). In fact the modified exponential relation (Eq. (8)) seems to provide the best prediction of the measured porosity dependence. This finding confirms earlier results with another, high-purity, submicron alumina type (AA04, Sumitomo, Japan),[13] as well as zirconia (TZ-3YE, Tosoh, Japan),[13] alumina–zirconia composites with 20 wt.% alumina (TZ-3Y20A, Tosoh, Japan),[45] kaolinite-based refractories[65] and porous mullite materials,[31] all prepared with fugitive biogenic pore-forming agents (see Fig. 2).

With respect to the estimated error of measurement (approximately 5%), no pore size dependence could be detected, although the pore sizes investigated in the present work extend about approximately one order of magnitude (median values approximately 5 μm resulting from rice starch and approximately 50 μm resulting from potato starch).[41]

Figs. 3 and 4 show the measured temperature dependence of the thermal conductivity of porous alumina ceramics prepared by traditional slip casting with different starch types from room temperature to approximately 500 °C. The thick full curve in these two graphs is based on literature data (including recent ones) concerning dense alumina ceramics (with a porosity below 3%) and can be expressed by the empirical relation[45]

$$k_0 = 3645(\vartheta + 194)^{-0.874}, \qquad (12)$$

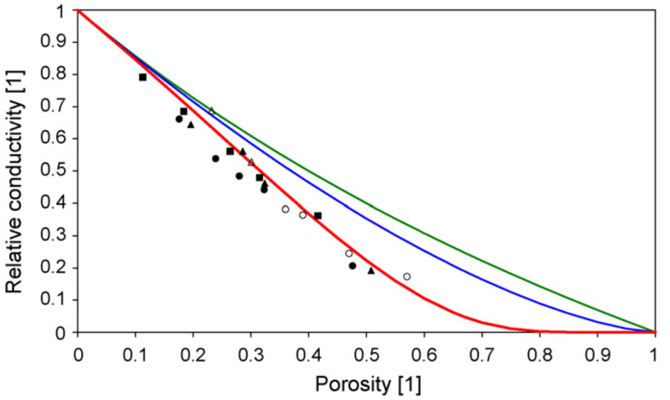

Fig. 2. Porosity dependence of the relative thermal conductivity of porous ceramics prepared by starch-consolidation casting (full squares zirconia; full circles, alumina; full triangles, alumina–zirconia composites) and other shaping techniques with bioorganic pore-forming agents (empty triangles, kaolinite-based refractories; empty circles, mullite materials), compared to the HS upper bound (top curve), the power-law relation (middle curve), and the modified exponential relation (bottom curve); literature data.[13,45,65,67]

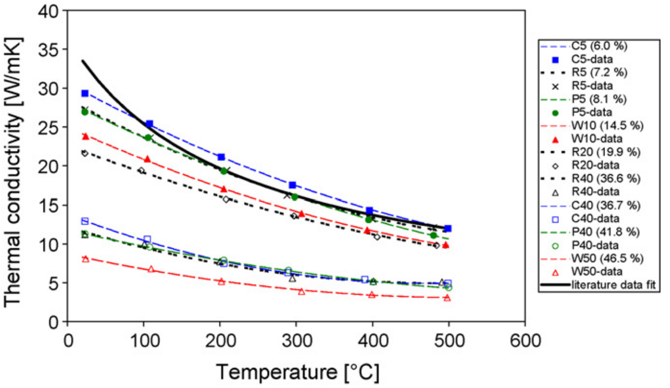

Fig. 3. Temperature dependence of the thermal conductivity of porous alumina ceramics prepared by traditional slip casting (data for ceramics with different porosity and pore size, i.e. starch types/squares, corn; three dotted curves, rice; circles, potato; triangles, wheat; fitted with second-order polynomials), compared to the fit curve for alumina ceramics based on literature data (thick full curve).

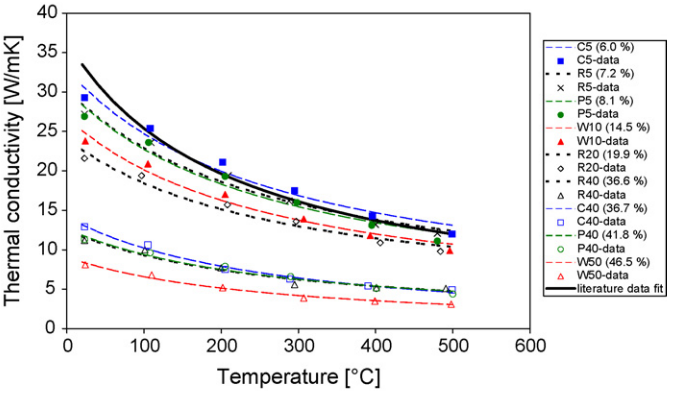

Fig. 4. Temperature dependence of the thermal conductivity of porous alumina ceramics prepared by traditional slip casting; data for ceramics with different porosity and pore size, i.e. starch types/squares, corn; three dotted curves, rice; circles, potato; triangles, wheat; fitted with the relation $k_r = A + B/(\vartheta + 273)$, compared to the fit curve for alumina ceramics based on literature data.

where ϑ is the temperature value in °C. It is in very close agreement with the empirical temperature dependence interpolation formula proposed for dense alumina by Munro,[55] which is

$$k_0 = 5.85 + \frac{15360\,\exp(-0.002\vartheta)}{\vartheta + 516}, \tag{13}$$

where ϑ is also the temperature value in °C and the estimated error is ±6%. Although our measured values exhibit a reasonable and consistent trend with porosity (highest for porosities of 6–8%, intermediate for approximately 15–20% and lowest for 37–47%), it is obvious that in the temperature range between 100 and 400 °C our values are slightly higher than expected and our overall temperature dependence is slightly less curved than the dependences corresponding to Eqs. (12) and (13). The definite reason for these differences is not clear (a small content of glassy grain boundary phase might explain the decreased curvature, but not the higher absolute values; moreover, the occurrence of a significant glassy grain boundary phase can be excluded with respect to the purity of the alumina powder used), and since we cannot find any error in our approach the data obtained may stand as they are (note that the interpolation formula in Munro's review, Eq. (13), is based on a relatively weak data base of only three papers, two of them published before 1966, while our fit, Eq. (12), additionally includes only a few values more, some from a classic Kingery paper,[66] and some from a more recent paper by Nieto et al.[67]).

In order to obtain the values at exactly 100, 300 and 500 °C the measured data had to be interpolated using appropriate fit relations (dashed or dotted curves in Figs. 3 and 4). In Fig. 3 fitting has been performed using the second-order polynomial

$$k = a + b\vartheta + c\vartheta^2, \tag{14}$$

while in Fig. 4 the data have been fitted via the inverse-absolute-temperature relation[54,56]

$$k = A + \frac{B}{(\vartheta + 273)}. \tag{15}$$

The resulting values of the fit parameters are listed in Tables 1 and 2, together with the corresponding correlation coefficients. It is evident that the temperature dependence of the thermal conductivity can be fitted by the inverse-absolute-temperature relation (correlation coefficient > 0.98), as expected from theory for crystalline materials.[52,54] However, the second-order polynomial fit, although only empirical, represents a closer fit (correlation coefficient > 0.99) (see Figs. 3 and 4), obviously due to the presence of an additional fit parameter. It has to be noted, of course, that the second-order polynomial cannot be used beyond the range of measured values, because it may result in numerical artifacts such as negative conductivities for higher temperatures (in contrast to Eq. (15), which may – with due caution – be used for higher temperatures and extrapolation purposes).

Table 1

Fit parameters a, b, c of the temperature dependence of thermal conductivity (with correlation coefficient R), according to the empirical second-order polynomial fit relation (Eq. (14))

Sample label	Porosity (%)	a	b	c	R
C 5	6.0	30.7	−0.0542	3.34×10^{-5}	0.9998
R 5	7.2	28.6	−0.0533	3.83×10^{-5}	0.999
P 5	8.1	28.2	−0.0484	2.65×10^{-5}	0.9997
W 10	14.5	25.0	−0.0446	2.83×10^{-5}	0.9996
R 20	19.9	22.6	−0.0368	2.11×10^{-5}	0.999
R 40	36.6	12.2	−0.0298	3.06×10^{-5}	0.990
C 40	36.7	13.8	−0.0375	3.96×10^{-5}	0.998
P 40	41.8	11.8	−0.0225	1.51×10^{-5}	0.9997
W 50	46.5	8.7	−0.0213	2.02×10^{-5}	0.998

Table 2

Fit parameters A and B of the temperature dependence of thermal conductivity (with correlation coefficient R), according to the inverse-temperature fit relation (Eq. (15))

Sample label	Porosity (%)	A	B	R
C 5	6.0	2.25	8383	0.986
R 5	7.2	2.54	7613	0.988
P 5	8.1	1.91	7767	0.984
W 10	14.5	1.88	6813	0.987
R 20	19.9	2.82	5829	0.985
R 40	36.6	0.50	3287	0.981
C 40	36.7	−0.64	4049	0.994
P 40	41.8	0.40	3360	0.988
W 50	46.5	−0.24	2546	0.993

Figs. 5 and 6 show the data obtained by interpolation with Eqs. (14) and (15), respectively, compared to the porosity dependence predicted by the modified exponential relation, Eq. (8), using the temperature dependence of k_0 based on independent literature data, Eq. (12). We emphasize that these curves (for room temperature, 100, 300 and 500 °C, respectively, from top to bottom) represent parameter-free predictions, constructed completely independently from the experimental results of this paper (i.e. without prior knowledge of the measured data). Therefore the agreement with the measured data has to be considered as more than satisfactory (note that, using the temperature dependence experimentally measured in this paper, arbitrarily good agreement could be achieved). This confirms that the modified exponential relation, Eq. (8), provides a useful prediction for

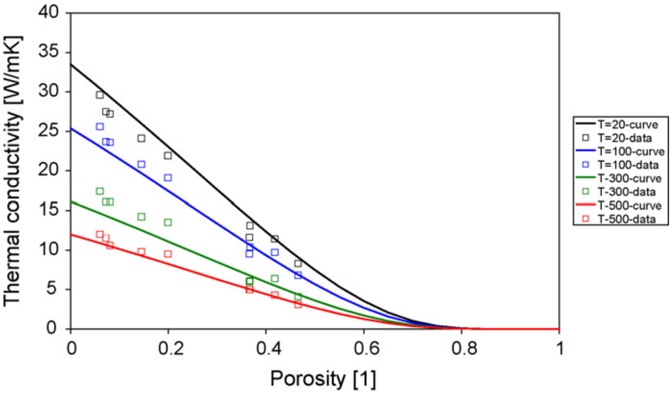

Fig. 5. Porosity dependence of the thermal conductivity of alumina ceramics prepared by traditional slip casting at different temperatures (from top to bottom: 20, 100, 300, 500 °C); values interpolated from Fig. 3 (using Eq. (14) and Table 1).

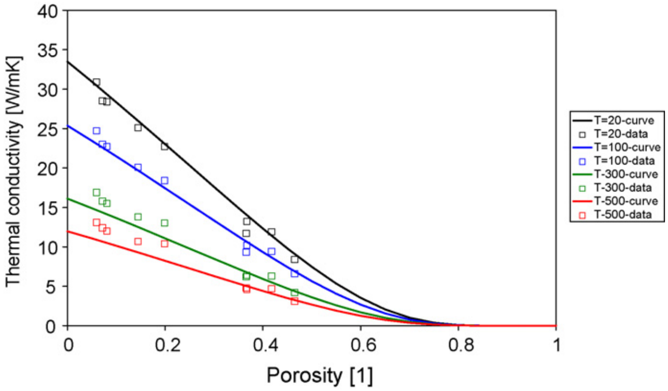

Fig. 6. Porosity dependence of the thermal conductivity of alumina ceramics prepared by traditional slip casting at different temperatures (from top to bottom: 20, 100, 300, 500 °C); values interpolated from Fig. 4 (using Eq. (15) and Table 2).

the effective thermal conductivity not only at room temperature but also at higher temperature, as long as radiation effects are insignificant.

5. Conclusion

The thermal conductivity of porous alumina ceramics prepared using different types of starch (potato, wheat, corn, and rice starch) as pore-forming agents has been investigated from room temperature up to 500 °C. The temperature dependence measured for alumina ceramics of different porosity (6–47%) is fitted with second-order polynomials and $1/T$-type relations and compared to available literature data for dense alumina. To our knowledge, these are the first systematic measurements of the combined temperature and porosity dependence of porous alumina ceramics prepared using pore-forming agents. The $1/T$ dependence has been roughly confirmed for all porosities, although second-order polynomials were shown to give better fits (correlation coefficients >0.99 versus 0.98–0.99 for the $1/T$ fits). The most important result of this paper, however, is the finding that the porosity dependence of the relative thermal conductivity $k_r = k/k_0$ is well described by a modified exponential relation of the form $k_r = \exp(-1.5\phi/(1-\phi))$, where ϕ is the porosity. This finding is in agreement with other literature data and seems to indicate a common feature of all porous materials with microstructures resulting from fugitive pore-forming agents, which leave essentially convex pores after burnout and firing. The porosity dependence predicted with the modified exponential relation is in very good agreement with the measured values at room temperature, and even for elevated temperatures (up to 500 °C) this parameter-free prediction yields a satisfactory a priori estimate of the measured values, especially for high porosities. Within the pore size range studied here (median pore sizes in the range 5–50 μm, i.e. order of magnitude approximately 1–100 μm) no pore size dependence could be observed. However, a pore-size dependence must be expected beyond this size range, in particular at higher temperatures (where radiation may become significant) and porosities (when the degree of open porosity permits convective heat transfer).

Acknowledgement

This study was part of the project IAA401250703 “Porous ceramics, ceramic composites and nanoceramics”, supported by the Grant Agency of the Academy of Sciences of the Czech Republic.

References

1. Rice, R. W., *Porosity of Ceramics*. Marcel Dekker, New York, 1998, pp. 315–532.
2. Scheffler, M. and Colombo, P., ed., *Cellular Ceramics—Structure, Manufacturing, Properties and Applications*. Wiley–VCH, Weinheim, 2005. pp. 342–360, 401–620.
3. Torquato, S., *Random Heterogeneous Materials—Microstructure and Macroscopic Properties*. Springer, New York, 2002, pp. 1–701.
4. Markov, K. Z., Elementary micromechanics of heterogeneous media. In *Heterogeneous Media—Micromechanics Modeling Methods and Simulations*, ed. K. Markov and L. Preziosi. Birkhäuser, Boston, 2000, pp. 1–162.
5. Pabst, W. and Gregorová, E., Cross-property relations between elastic and thermal properties of porous ceramics. *Adv. Sci. Technol.*, 2006, **45**, 107–112.
6. Pabst, W. and Gregorová, E., A cross-property relation between the tensile modulus and the thermal conductivity of porous materials. *Ceram. Int.*, 2007, **33**, 9–12.
7. Pabst, W., Gregorová, E. and Tichá, G., Effective properties of suspensions, composites and porous materials. *J. Eur. Ceram. Soc.*, 2007, **27**, 479–482.
8. Pabst, W. and Gregorová, E., Effective elastic properties of alumina-zirconia composite ceramics. Part 2: Micromechanical modeling. *Ceramics-Silikáty*, 2004, **48**, 14–23.
9. Pabst, W. and Gregorová, E., Mooney-type relation for the porosity dependence of the tensile modulus of ceramics. *J. Mater. Sci.*, 2004, **39**, 3213–3215.
10. Pabst, W., Gregorová, E., Tichá, G. and Týnová, E., Effective elastic properties of alumina-zirconia composite ceramics. Part 4: Tensile modulus of porous alumina and zirconia. *Ceramics-Silikáty*, 2004, **48**, 165–174.
11. Pabst, W., Tichá, G., Gregorová, E. and Týnová, E., Effective elastic properties of alumina-zirconia composite ceramics. Part 5: Tensile modulus of alumina-zirconia composite ceramics. *Ceramics-Silikáty*, 2005, **49**, 77–85.
12. Pabst, W., Tichá, G. and Gregorová, E., Thermal conductivity of ceramic composites and porous ceramics. In *Proceedings of the International Conference on Porous Ceramic Materials*, ed. J. Luyten and F. Snijkers. VITO Materials Technology, Mol, 2005, 6 pp. in CD.
13. Tichá, G., Pabst, W. and Smith, D. S., Predictive model for the thermal conductivity of porous materials with matrix-inclusion type microstructure. *J. Mater. Sci.*, 2005, **40**, 5045–5047.
14. Rice, R. W., *Ceramic Fabrication Technology*. Marcel Dekker, New York, 2003, pp. 283–302.
15. Studart, A. R., Gonzenbach, T., Tervoort, E. and Gauckler, L. J., Processing routes to macroporous ceramics: a review. *J. Am. Ceram. Soc.*, 2006, **89**, 1771–1789.
16. Živcová, Z., Gregorová, E. and Pabst, W., Alumina ceramics prepared with new pore-forming agents. *Proc. Appl. Ceram.*, 2008, **2**, 1–8.
17. Lyckfeldt, O. and Ferreira, J. M. F., Processing of porous ceramics by “starch consolidation”. *J. Eur. Ceram. Soc.*, 1998, **18**, 131–140.
18. Alves, H. M., Tarí, G., Fonseca, A. T. and Ferreira, J. M. F., Processing of porous cordierite bodies by starch consolidation. *Mater. Res. Bull.*, 1998, **33**, 1439–1448.
19. Corbin, S. F. and Apte, P. S., Engineered porosity via tape casting, lamination and the percolation threshold of pyrolyzable particulates. *J. Am. Ceram. Soc.*, 1999, **82**, 1693–1701.
20. Davis, J., Kristoffersson, A., Carlström, E. and Clegg, W., Fabrication and crack deflection in ceramic laminates with porous interlayers. *J. Am. Ceram. Soc.*, 2000, **83**, 2369–2374.
21. Lemos, A. F. and Ferreira, J. M. F., Porous bioactive calcium carbonate implants processed by starch consolidation. *Mater. Sci. Eng.*, 2000, **C11**, 35–40.

22. Pabst, W., Gregorová, E., Havrda, J. and Týnová, E., Gelatin casting and starch consolidation of alumina ceramics. In *Ceramic Materials and Components for Engines*, ed. J. G. Heinrich and F. Aldinger. Wiley–VCH, Weinheim, 2001, pp. 587–592.
23. Týnová, E., Pabst, W., Gregorová, E. and Havrda, J., Starch consolidation casting of alumina ceramics—body formation and microstructural characterization. *Key Eng. Mater.*, 2002, **206–213**, 1969–1972.
24. Bowden, M. E. and Rippey, M. S., Porous ceramics formed using starch consolidation. *Key Eng. Mater.*, 2002, **206–213**, 1957–1960.
25. Galassi, C., Roncari, E., Capiani, C., Fabbri, G., Piancastelli, A., Peselli, M. and Silvano, F., Processing of porous PZT materials for underwater acoustics. *Ferroelectrics*, 2002, **268**, 47–52.
26. Kim, J. G., Sim, J. H. and Cho, W. S., Preparation of porous (Ba,Sr)TiO_3 by adding corn-starch. *J. Phys. Chem. Solids*, 2002, **63**, 2079–2084.
27. Kim, J. G., Cho, W. S. and Sim, J. H., Effect of potato-starch on the microstructure and PTCR characteristics of (Ba,Sr)TiO_3. *J. Mater. Sci. Mater. Electron.*, 2002, **13**, 497–501.
28. Díaz, A. and Hampshire, S., Characterization of porous silicon nitride materials produced with starch. *J. Eur. Ceram. Soc.*, 2004, **24**, 413–419.
29. Mattern, A., Huchler, B., Staudenecker, D., Oberacker, R., Nagel, A. and Hoffmann, M. J., Preparation of interpenetrating ceramic–metal composites. *J. Eur. Ceram. Soc.*, 2004, **24**, 3399–3408.
30. Reynaud, C., Thévenot, F., Chartier, T. and Besson, J.-L., Mechanical properties and mechanical behaviour of SiC dense-porous laminates. *J. Eur. Ceram. Soc.*, 2005, **25**, 589–597.
31. Barea, R., Osendi, M. I., Ferreira, J. M. F. and Miranzo, P., Thermal conductivity of highly porous mullite material. *Acta Mater.*, 2005, **53**, 3313–3318.
32. Galassi, C., Processing of porous ceramics—piezoelectric materials. *J. Eur. Ceram. Soc.*, 2006, **26**, 2951–2958.
33. García-Gabaldón, M., Pérez-Herranz, V., Sánchez, E. and Mestre, S., Effect of porosity on the effective electrical conductivity of different ceramic membranes used as separators in electrochemical reactors. *J. Membr. Sci.*, 2006, **280**, 536–544.
34. Romano, P., Velasco, F. J., Torralba, J. M. and Candela, N., Processing of M2 powder metallurgy high-speed steel by means of starch consolidation. *Mater. Sci. Eng. A*, 2006, **419**, 1–7.
35. LeBeau, J. M. and Boonyongmaneerat, Y., Comparison study of aqueous binder systems for slurry-based processing. *Mater. Sci. Eng. A*, 2007, **458**, 17–24.
36. Yang, L., Ning, X., Chen, K. and Zhou, H., Preparation and properties of hydroxyapatite filters for microbial filtration. *Ceram. Int.*, 2007, **33**, 483–489.
37. Sopyan, I., Mel, M., Ramesh, S. and Khalid, K. A., Porous hydroxyapatite for artificial bone applications. *Sci. Technol. Adv. Mater.*, 2007, **8**, 116–123.
38. Gregorová, E. and Pabst, W., Porosity and pore size control in starch consolidation casting—achievements and problems. *J. Eur. Ceram. Soc.*, 2007, **27**, 669–672.
39. Bhattacharjee, S., Besra, L. and Singh, B. P., Effect of additives on the microstructure of porous alumina. *J. Eur. Ceram. Soc.*, 2007, **27**, 47–52.
40. Mao, X., Wang, S. and Shimai, S., Porous ceramics with tri-modal pores prepared by foaming and starch consolidation. *Ceram. Int.*, 2008, **34**, 107–112.
41. Gregorová, E., Pabst, W. and Bohačenko, I., Characterization of different starch types for their application in ceramic processing. *J. Eur. Ceram. Soc.*, 2006, **26**, 1301–1309.
42. Gibson, L. J. and Ashby, M. F., *Cellular Solids—Structure and Properties* (*2nd edition*). Cambridge University Press, Cambridge, 1997, pp. 283–295.
43. Loeb, A. L., Thermal conductivity VIII—a theory of thermal conductivity of porous materials. *J. Am. Ceram. Soc.*, 1954, **37**, 96–99.
44. Francl, J. and Kingery, W. D., Thermal conductivity IX—experimental investigation of the effect of porosity on thermal conductivity. *J. Am. Ceram. Soc.*, 1954, **37**, 99–107.
45. Pabst, W. and Gregorová, E., Effective thermal and thermoelastic properties of alumina, zirconia and alumina–zirconia composite ceramics. In *New Developments in Materials Science Research*, ed. B. M. Caruta. Nova Science Publishers, New York, 2007, pp. 77–137.
46. Weast, R. C., *CRC Handbook of Chemistry and Physics. 1st Student's Edition*. CRC Press, Boca Raton, 1988, pp. E2, F10–F12.
47. Landauer, R., The electrical resistance of binary metallic mixtures. *J. Appl. Phys.*, 1952, **23**, 779–784.
48. Bruggeman, D. A. G., Berechnung verschiedener physikalischer Konstanten von heterogenen Stoffen. I. Dielektrizitätskonstanten und Leitfähigkeiten der Mischkörper aus isotropen Substanzen. *Ann. Physik Leipzig*, 1935, **24**, 636–679.
49. Pabst, W., Gregorová, E. and Tichá, G., Elasticity of porous ceramics—a critical study of modulus-porosity relations. *J. Eur. Ceram. Soc.*, 2006, **26**, 1085–1097.
50. Pabst, W. and Gregorová, E., Derivation of the simplest exponential and power-law relations for the effective tensile modulus of porous ceramics via functional equations. *J. Mater. Sci. Lett.*, 2003, **22**, 1673–1675.
51. Hristopulos, D. T. and Demertzi, M., A semi-analytical equation for the Young's modulus of isotropic ceramic materials. *J. Eur. Ceram. Soc.*, 2008, **28**, 1111–1120.
52. Schlichting, K. W., Padture, N. P. and Klemens, P. G., Thermal conductivity of dense and porous yttria-stabilized zirconia. *J. Mater. Sci.*, 2001, **36**, 3003–3010.
53. Kingery, W. D. and McQuarrie, M. C., Thermal conductivity I—concepts of measurement and factors affecting thermal conductivity of ceramic materials. *J. Am. Ceram. Soc.*, 1954, **37**, 67–72.
54. Kingery, W. D., Bowen, H. K. and Uhlmann, D. R., *Introduction to Ceramics* (*2nd edition*). Wiley, New York, 1976, pp. 581–645.
55. Munro, R. G., Evaluated material properties for a sintered α-alumina. *J. Am. Ceram. Soc.*, 1997, **80**, 1919–1928.
56. Dos Santos, W. N., Effect of moisture and porosity on the thermal properties of a conventional refractory concrete. *J. Eur. Ceram. Soc.*, 2003, **23**, 745–755.
57. Smith, D. S., Fayette, S., Grandjean, S., Martin, C., Telle, R. and Tonnessen, T., Thermal resistance of grain boundaries in alumina ceramics and refractories. *J. Am. Ceram. Soc.*, 2003, **86**, 105–111.
58. Smith, D. S., Grandjean, S., Absi, J., Kadiebu, S. and Fayette, S., Grain-boundary thermal resistance in polycrystalline oxides: alumina, tin oxide, and magnesia. *High Temp. High Press.*, 2003/2004, **35/36**, 93–99.
59. Poulier, C., Smith, D. S., Demjan, J. and Absi, J., Porous oxide ceramics for thermal insulation: the role of interfaces on heat transfer. In *Proceedings of the International Conference on Porous Ceramic Materials*, ed. J. Luyten and F. Snijkers. VITO Materials Technology, Mol, 2005, 6 pp. in CD.
60. Poulier, C., Smith, D. S. and Absi, J., Thermal conductivity of pressed power compacts: tin oxide and alumina. *J. Eur. Ceram. Soc.*, 2007, **27**, 475–478.
61. Gregorová, E., Živcová, Z., Pabst, W. and Sedlářová, I., Characterization of porous ceramics by image analysis and mercury porosimetry. *Ceramika-Ceramics*, 2006, **97**, 219–230.
62. Gregorová, E., Živcová, Z. and Pabst, W., Porosity and pore space characteristics of starch-processed porous ceramics. *J. Mater. Sci.*, 2006, **41**, 6119–6122.
63. Parker, W. J., Jenkins, R. J., Butler, C. P. and Abbot, G. L., Flash method of determining thermal diffusivity, heat capacity, and thermal conductivity. *J. Appl. Phys.*, 1961, **32**, 1679–1684.
64. Degiovanni, A., Diffusivité et méthode flash. *Rev. Gen. Therm. (France)*, 1977, **185**, 420–441.
65. Ogacho, A. A., Aduda, B. O. and Nyonesa, F. W., Thermal conductivity of a kaolinite refractory: effect of a plant-derived organic binder. *J. Mater. Sci.*, 2003, **38**, 2293–2297.
66. Kingery, W. D., Francl, J., Coble, R. L. and Vasilos, T., Thermal conductivity X—data for several pure oxide materials corrected to zero porosity. *J. Am. Ceram. Soc.*, 1954, **37**, 107–110.
67. Nieto, M. I., Martínez, R., Mazerolles, L. and Baudín, C., Improvement in the thermal shock resistance of alumina through the addition of submicron-sized aluminium nitride particles. *J. Eur. Ceram. Soc.*, 2004, **24**, 2293–2301.